



First-principle calculations of Co_2MSi (M=Cr, Mn, Fe) Heusler alloys

Ashish Pathak* • R. Sankarasubramanian

Defence Metallurgical Research Laboratory, Kanchanbagh P.O., Hyderabad – 500058

Received 03 14 2022; accepted 03 09 2022

Available 06 30 2022

Abstract: The present work describes the electronic structure, magnetic and elastic properties of ordered Co_2MSi (M = Cr, Mn, Fe) Heusler alloys in $L2_1$ structure calculated using density functional theory within generalized gradient approximation. The calculated band structures, density of states and magnetic moments have been discussed. The magnetic moment values obtained in present study follow the Slater-Pauling rule. A small band gap in the minority band structure at the Fermi level suggests half-metallicity. Hundred percentage spin polarization in this ordered structure implies that these materials possess ferromagnetism. All the three materials satisfy stability criteria in terms of elastic constants and are predicted to have ductile behavior based on the ratio of shear to bulk modulus.

Keywords: Density-functional theory, electronic structure, magnetism, elastic properties

*Corresponding author.

E-mail address: ashishpathak1980@gmail.com (Ashish Pathak).

Peer Review under the responsibility of Universidad Nacional Autónoma de México.

1. Introduction

Ternary intermetallic alloys with X_2YZ stoichiometric composition are known as full Heusler alloys. These materials have attracted attention due to several properties such as half-metallicity, ferromagnetism, magnetocaloric, magneto-optical, thermoelectricity, ferromagnetic shape memory effect, etc. Heusler alloys with space group $Fm\bar{3}m$ (No. 225) crystallize in ordered $L2_1$ structure with face centred cubic (fcc) unit cell. In these compounds, X and Y are generally high and low valence transition metal atoms, respectively and Z is an element with s-p type valence electrons (Graf et al., 2011; Galanakis & Mavropoulos, 2007; Luo et al., 2007).

Recently, structural and magnetic properties of Co_2FeSi thin films and $Co_2FeSi_{1-x}B_x$ Heusler alloys have been reported by Hazra et al. (2016) and Ramudu et al. (2015), respectively. The magnetic properties of Co_2CrSi , Co_2MnSi and Co_2FeSi have been previously studied (Antonov et al., 2008; Kandpal et al., 2006; Kumar et al., 2009; Rai et al., 2011). However, they have not addressed the mechanical properties of these magnetic alloys which is an important factor for handling the component made of these alloys. In the present work, electronic structural, magnetic and mechanical properties of Co_2MSi ($M = Cr, Mn, Fe$) Heusler alloys have been investigated using the density-functional theory (DFT) approach.

Recently, Mohankumar et al. (2015) reported the half-metallic property of disordered B2 structure of Co_2FeSi . They have also described that the half-metallicity vanishes at the moderate percentage of B2 disorders due to the creation of new states at the Fermi level (E_F) in the minority density of states (DOS) but at low and high levels of disorders, the half-metallicity has been retained. Further, Seema et al. (2015) studied the effect of disorder on the electronic, magnetic and optical properties of Co_2CrZ ($Z = Al, Ga, Si, Ge$) Heusler alloys and Guezlane et al. and Amari et al. have studied $Co_2Cr_xFe_{1-x}X$ ($X = Al, Si$) and $Co_2FeGe_{1-x}Si_x$ ($x = 0, 0.5, 1$) Heusler alloys using first-principle calculations (Amari et al., 2016; Guezlane et al., 2016).

Present work is thus concerned with a comprehensive and consistent approach to explore the electronic structure, single crystal elastic and polycrystalline bulk mechanical properties of ordered Co_2MSi ($M = Cr, Mn, Fe$) Heusler alloys in $L2_1$ structure using first-principle total energy calculations. The results obtained in the present study have been compared with experimental and theoretical values wherever available.

2. Methodology

The DFT calculations (Hohenberg & Kohn, 1964; Kohn & Sham, 1965) have been executed using Vienna ab initio simulation package (VASP) ([Cms.mpi.univie.ac.at/vasp/](http://cms.mpi.univie.ac.at/vasp/)) to study the electronic structure, magnetic and elastic properties of the Heusler alloys. The projected augmented plane wave (PAW)

pseudopotential and generalized gradient approximations (GGA) have been utilized for exchange correlation energy with the Perdew-Burke-Ernzerhof (PBE) function (Perdew et al., 1996). It is well known that the local density approximations (LDA) or the generalized gradient approximations (GGA) functions underestimate the energy band gaps and can give smaller or less than fifty percentage energy band gaps. Lack of derivative discontinuity as well as an incomplete self-interaction cancellation in the GGA exchange correlation (xc) functional are the main reasons behind the reduced/ incorrect band gap estimate. Therefore, to overcome these difficulties, more appropriate green function (GW_0) (Hedin, 1965), modified Becke-Jonson (mBJ) (Tran & Blaha, 2009) and Heyd-Seuseria-Ernzerhof (HSE) (Heyd et al., 2003) methods have also been performed for the electronic structure calculations.

A plane-wave cut-off energy of 268 eV has been used after checking the convergence (Fig 1(a)). For Brillouin zone (BZ) integration, a k-point mesh based on the convergence test is used (Fig 1(b)), which is corresponding to $10 \times 10 \times 10$ Monkhorst-Pack mesh (Monkhorst & Pack, 1976). The lattice constants have been relaxed in all the three perpendicular axes to get the minimum energy of the system which is required for the structural optimization. Relaxation is terminated until the differences between energies or forces in two consecutive steps are less than 1×10^{-5} eV and $0.02 \text{ eV}/\text{\AA}$, respectively.

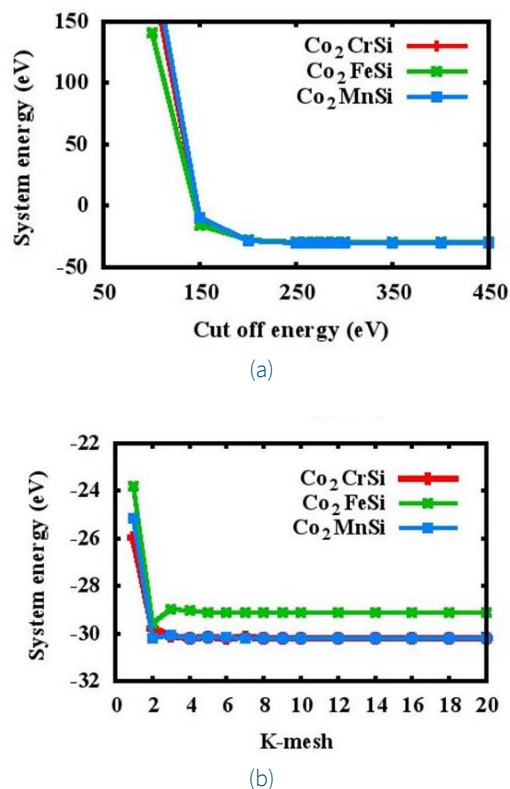


Figure 1. Convergence test (a) w.r.t cut off kinetic energy (b) w.r.t k-mesh.

The elastic constants have been calculated using the linear-response method implemented in VASP software. In this method, the second derivative of the total energy with respect to the strain has been utilized to calculate the elastic constants.

A schematic of the crystal structure of Co₂FeSi in L₂₁ ordered structure has been shown in Fig. 2. The unit cell consists of four atoms in a face centered cubic (fcc) cell with the atomic positions of Co at (1/4, 1/4, 1/4) and (3/4, 3/4, 3/4), Fe at (1/2, 1/2, 1/2) and Si at (0, 0, 0) in Wyckoff coordinates. The corresponding space group is Fm $\bar{3}$ m (No. 225).

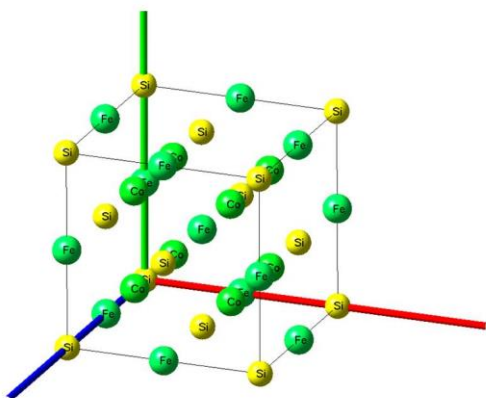


Figure 2. Crystal structure of ordered L₂₁ structure of Co₂FeSi Heusler alloy.

In general, Slater-Pauling rule has been followed by the d-block elements and their alloys in terms of the total spin magnetic moment (m_{total}) (Pauling, 1938; Slater, 1936). The net magnetic moment of a magnetic material can be defined as a difference between occupancy of valence electrons in the majority and minority spin states and is given by the relation.

$$m_H = N_v - 24 \quad (1)$$

where, N_v represents the total number of valence electrons and 24 represents twice the number of electrons in the minority state (Mohankumar et al., 2015). The total number of valence electrons (N_v) is ($2 \times 9 + 6 + 4 = 28$) 28 in Co₂CrSi and hence the total magnetic moment is $4 \mu_B$ (Kandpal et al., 2006). Similarly, the values of N_v for the Co₂MnSi and Co₂FeSi are 29 and 30, respectively. Therefore, the values m_H are 5 and $6 \mu_B$ for Co₂MnSi and Co₂FeSi, respectively. Further, a more common description for computing the spin polarization (P) is defined as (Pauling, 1938).

$$P = \frac{\rho \uparrow(E_F) - \rho \downarrow(E_F)}{\rho \uparrow(E_F) + \rho \downarrow(E_F)} \quad (2)$$

where $\rho \uparrow(E_F)$ and $\rho \downarrow(E_F)$ indicate majority and minority spin density of states at the Fermi level (E_F). This model suggests that the half-metallic ferro-magnets exhibit 100 % spin polarization at the Fermi level.

3. Results and discussion

Calculated lattice constants, site resolved magnetic moment, total magnetic moment, and spin polarization of L₂₁ ordered Co₂MSi (M = Cr, Mn and Fe) Heusler alloys are summarized in Tables 1–2.

Table 1. Equilibrium lattice constants (a) for Co₂MSi (M= Cr, Mn, Fe). The experimental and other available theoretical values are also given for comparison (Alhaj et al., 2013; Amari et al., 2016; Antonov et al., 2008; Guezlane et al., 2016; Kandpal et al., 2006; Rai et al., 2011; Raphael et al., 2002; Seema et al., 2015; Niculescu et al., 1977; Umetsu et al., 2014; Wurmehl et al., 2005; Yin et al., 2013; Zhu et al., 2014)

System	Lattice constant (Å)		
	Experimental	Theoretical	Present study
Co ₂ CrSi	5.65 ^a	5.699 ^b , 5.645 ^c , 5.634 ^d , 5.657 ^e	5.659
Co ₂ MnSi	5.654 ^f	5.651 ^g , 5.627 ^d	5.655
Co ₂ FeSi	5.658 ^h , 5.64 ⁱ , 5.636 ^j	5.545 ^k , 5.63 ^g , 5.634 ^c , 5.618 ^l , 5.578 ^m , 5.631 ^m	5.640

Ref.

^a(Umetsu et al., 2014)

^b(Rai et al., 2011)

^c(Guezlane et al., 2016)

^d(Alhaj et al., 2013)

^e(Seema et al., 2015)

^f(Raphael et al., 2002)

^g(Kandpal et al., 2006)

^h(Niculescu et al., 1977)

ⁱ(Wurmehl et al., 2005)

^j(Yin et al., 2013)

^k(Antonov et al., 2008)

^l(Zhu et al., 2014)

^m(Amari et al., 2016)

Lattice parameters of all the three alloys calculated in the present study are in good agreement with previously reported experimental and theoretical values (Alhaj et al., 2013; Amari et al., 2016; Antonov et al., 2008; Guezlane et al., 2016; Kandpal

et al., 2006; Niculescu et al., 1977; Rai et al., 2011; Raphael et al., 2002; Seema et al., 2015; Umetsu et al., 2014; Wurmehl et al., 2005; Yin et al., 2013; Zhu et al., 2014). It is well known that only Co and Cr/Mn/Fe atoms carry magnetic moments, while Si atom has a negative moment (Alhaj et al., 2013; Antonov et al., 2008; Chen et al., 2006; Guezlane et al., 2016; Kandpal et al., 2007; Kandpal et al., 2006; Rai et al., 2011; Raphael et al., 2002; Seema et al., 2015; Niculescu et al., 1977; Wurmehl et al., 2005). In the present study, the total magnetic moment for Co₂CrSi; Co₂MnSi and Co₂FeSi using (GGA, GW₀, mBJ and HSE06) approximations are estimated to be (3.934, 4.005, 4.000 and 4.000) μ_B; (4.990, 4.991, 5.000 and 5.019) μ_B and (5.521, 5.640, 5.8546 and 6.000) μ_B, respectively (Table 2). The values of total magnetic moment for these alloys are in accordance with the Slater-Pauling rule and agree with previously reported theoretical and experimental values (Antonov et al., 2008; Alhaj et al., 2013; Chen et al., 2006; Guezlane et al., 2016; Kandpal et al., 2006; Kandpal et al., 2007; Niculescu et al., 1977; Rai et al., 2011; Raphael et al., 2002; Seema et al., 2015; Wurmehl et al., 2005). It may be noted that the values calculated using HSE06 approximation are very close to the experimentally reported values (Table 2).

The band structures and density of states (DOS) for spin-up and spin-down for all the three alloys in GGA, GW₀, mBJ and HSE approximations have been calculated. The band structures and DOS for all the three alloys in GGA and HSE approximations are shown in Figs. 3–8. It is to be noted that up and down spin states are depicted using red and blue colours in the band structures. The total DOS are shown with black colour whereas the partial DOS are represented using different colours. The atomic contributions for M (M = Cr / Mn / Fe) atoms are higher than Co atom whereas the atomic contribution of Si atom is negligible. The atomic contributions are mainly due to Co (d), M(d) and Si(p) orbitals. The bonding in all the three alloys are due to Co(d)–M(d) atomic interactions.

It is clearly evident that the calculated DOS for all the three compounds show a half metallic behavior. The value of DOS at Fermi level (E_F) vanishes for the down-spin whereas shows finite values for the up-spin for Co₂CrSi. This reflects half-metallicity and ferromagnetism in Co₂CrSi. A similar behavior can be observed for Co₂MnSi and Co₂FeSi alloys. The band structure and DOS depict band gap in all the three alloys.

Calculated band gap for Co₂CrSi using GGA, GW₀, mBJ and HSE methods are 0.780, 0.860, 1.25 and 2.93 eV, respectively (Table 3). The calculated band gap value using GGA and mBJ are close to the other reported values (Alhaj et al., 2013; Chen et al., 2006; Guezlane et al., 2016; Rai et al., 2011; Seema et al., 2015). Similarly, band gap for Co₂MnSi using GGA, GW₀, mBJ and HSE methods are 0.720, 0.840, 1.74 and 2.78 eV, respectively (Table 3) and are in good agreement with earlier reported values (Antonov et al., 2008; Alhaj et al., 2013).

The band gap for Co₂FeSi using GGA; GW₀; mBJ and HSE methods are 0.680 (Γ–Γ); 0.820 (Γ–Γ); 1.95 (Γ–Γ), 0.86 (X–X); and 3.50(Γ–Γ), 2.23 eV (X–X); respectively (Table 3). The calculated band gap value using GGA and mBJ are close to the other reported values (Guezlane et al., 2016; Kandpal et al., 2006). It is to be noted that the band gaps for Co₂CrSi and Co₂MnSi alloys have been obtained for the Γ–Γ site symmetry whereas for Co₂FeSi alloy, it has been obtained for the X–X site symmetry also. Therefore, band gap for Co₂FeSi are given for both Γ–Γ and X–X site symmetries (Table 3).

Two-dimensional charge density distribution of all the three alloys in the (001) and (110) planes are shown in Figs. 9–11. All the three alloys display strong electronic interactions for Co-M and M-M type bonds whereas relatively weak interactions for the Co-Si and M-Si type bonds. The strong bonding is due to Co(d) and M(d) atomic interaction. All the Co₂MSi alloys show mixed metallic and covalent bonding.

The single crystal elastic properties for cubic materials are described by three independent elastic constants namely, C₁₁, C₁₂ and C₄₄ respectively and are given in Table 4. The nature of metallic bonding of cubic material can be predicted based on Cauchy pressures (C_p) (Pettifor & Aoki, 1991) which is defined as

$$C_P = C_{12} - C_{44} \quad (3)$$

The negative Cauchy pressure indicates more directional bonding whereas positive value means predominant metallic bonding. The calculated values of Cauchy pressures of all the alloys are positive (Table 5). Though charge density analysis indicates mixed metallic and covalent bonding, analysis based on Cauchy pressure clearly points towards the presence of predominantly metallic bonds in these alloys.

The values of elastic constants can be used to provide the information about the stability of these alloys. The Born stability criterion for cubic materials is given in equation (4) (Born, 1940; Fedorov, 1968).

$$S_1: C_{44} > 0, S_2: C_{11} - |C_{12}| > 0 \text{ and } S_3: C_{11} + 2C_{12} > 0 \quad (4)$$

The calculated elastic constants have been used to assess the stability of these alloys. Since all the criteria are satisfied for all the compounds, it can be concluded that they are mechanically stable (Table 4).

Zener anisotropy factor (A) for cubic materials is defined below.

$$A = \frac{2C_{44}}{(C_{11} - C_{12})} \quad (5)$$

Unity value of 'A' suggests elastically isotropic crystal while, any deviation from unity indicates anisotropy. The values of anisotropic factor (A) obtained in present study for these alloys are away from unity indicating that the Heusler alloys studied here are elastically anisotropic (Table 4). It may be noted that the extent of anisotropy is very high for Co₂MnSi followed by Co₂FeSi and Co₂CrSi alloys.

Table 2. Calculated magnetic moments (using GGA, GW₀, MBJ and HSE06) m_{Co} , m_M (M = Cr, Mn, Fe) and m_{Si} is in bohr magneton (μ_B) as well as DOS for spin up $\rho_{\uparrow}(E_F)$ and spin down $\rho_{\downarrow}(E_F)$ at fermi level and spin polarization (P) for Co₂MSi (M= Cr, Mn, Fe). The experimental and other available theoretical values are also given for comparison (Antonov et al., 2008; Alhaj et al., 2013; Chen et al., 2006; Guezlane et al., 2016; Kandpal et al., 2006; Kandpal et al., 2007; Niculescu et al., 1977; Rai et al., 2011; Raphael et al., 2002; Seema et al., 2015; Wurmehl et al., 2005).

System		Magnetic moment (μ_B)				Spin polarisation			
		m_{Co}	m_M	m_{Si}	m_{total}	$\rho_{\uparrow}(E_F)$	$\rho_{\downarrow}(E_F)$	P (%)	
Co ₂ CrSi	Present study								
	GGA	0.990	1.995	-0.041	3.934	5.000	0.000	100	
	GW ₀	0.997	1.973	-0.039	4.005			100	
	mbJ	1.000	1.968	-0.034	4.000			100	
	HSE06	0.997	2.312	-0.079	4.000			100	
	Others		0.980 ^a	2.102 ^a	-0.055 ^a	4.006 ^a			100 ^a
			0.953 ^c	2.258 ^c	-0.160 ^c	4.004 ^c			100 ^c
			1.000 ^d	2.030 ^d		4.006 ^d			100 ^d
	GGA ^b mbJ ^b		0.980 ^e	2.080 ^e		4.000 ^e			100 ^e
			1.02 ^b	1.85 ^b	-0.03 ^b	4.00 ^b			100 ^b
			1.13 ^b	1.85 ^b	-0.04 ^b	4.00 ^b			100 ^b
			1.02 ^f	1.90 ^f	-0.04 ^f	4.00 ^f			100 ^f
Co ₂ MnSi	Present study								
	GGA	1.033	2.968	-0.044	4.990	1.500	0.000	100	
	GW ₀	1.039	2.929	-0.039	4.991			100	
	mbJ	1.143	2.967	-0.057	5.000			100	
	HSE06	0.970	3.490	-0.099	5.019			100	
	Experimental				5.10 ^g				
	Others		1.029 ^k	3.058 ^k	-0.055 ^k	5.031 ^k			100 ^k
		1.07 ^f	2.87 ^f	-0.04 ^f	5.00 ^f			100 ^f	
Co ₂ FeSi	Present study								
	GGA	1.348	2.752	-0.003	5.521	1.800	0.000	100	
	GW ₀	1.396	2.841	-0.003	5.640			100	
	mbJ	1.531	2.944	0.011	5.8546			100	
	HSE06	1.494	3.232	-0.013	6.000			100	
	Experimental				6.00 ^h , 5.91 ⁱ				
	Others		1.224 ^j	2.709 ^j	-0.033 ^j	5.125 ^j			100 ^j
		GGA ^b	1.37 ^b	2.75 ^b	-0.003 ^b	5.47 ^b			100 ^b
		mbJ ^b	1.54 ^b	2.96 ^b	-0.002 ^b	5.84 ^b			100 ^b
GGA ^k		1.39 ^k	2.85 ^k		5.56 ^k			100 ^k	

Ref.

^a (Rai et al., 2011)

^b (Guezlane et al., 2016)

^c (Seema et al., 2015)

^d (Kandpal et al., 2007)

^e (Chen et al., 2006)

^f (Alhaj et al., 2013)

^g (Raphael et al., 2002)

^h (Wurmehl et al., 2005)

ⁱ (Niculescu et al., 1977)

^j (Antonov et al., 2008)

^k (Kandpal et al., 2006)

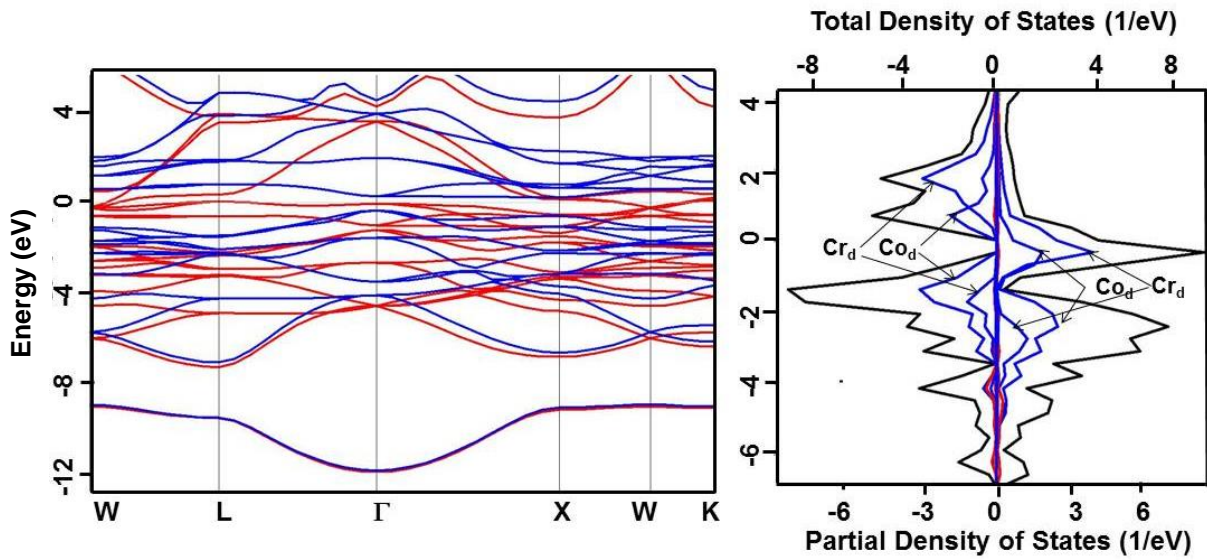


Fig 3 (a)

Fig 3 (b)

Figure 3. For Co_2CrSi alloy under GGA (a) Band structure. Up and down spin states have been represented using red and blue colours, respectively. (b) Total DOS (black) and partial DOS of individual atoms. Scales on the top and the bottom axes are to be used to read the total and partial DOS, respectively.

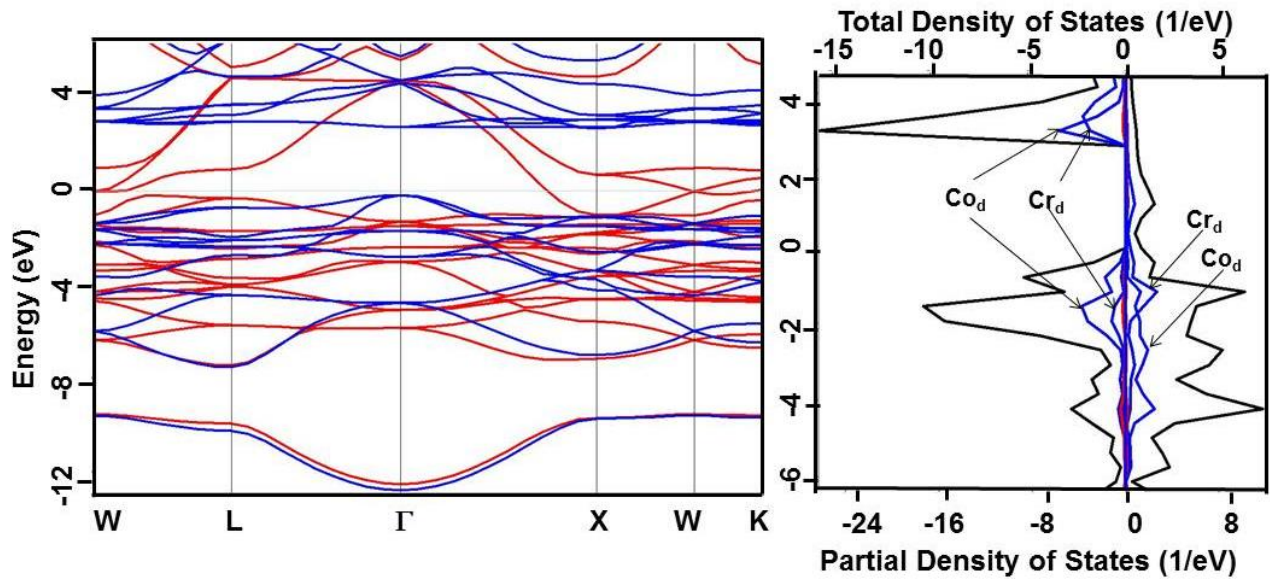


Fig 4 (a)

Fig 4(b)

Figure 4. For Co_2CrSi alloy under HSE approximation (a) Band structure. Up and down spin states have been represented using red and blue colours, respectively. (b) Total DOS (black) and partial DOS of individual atoms. Scales on the top and the bottom axes are to be used to read the total and partial DOS, respectively.

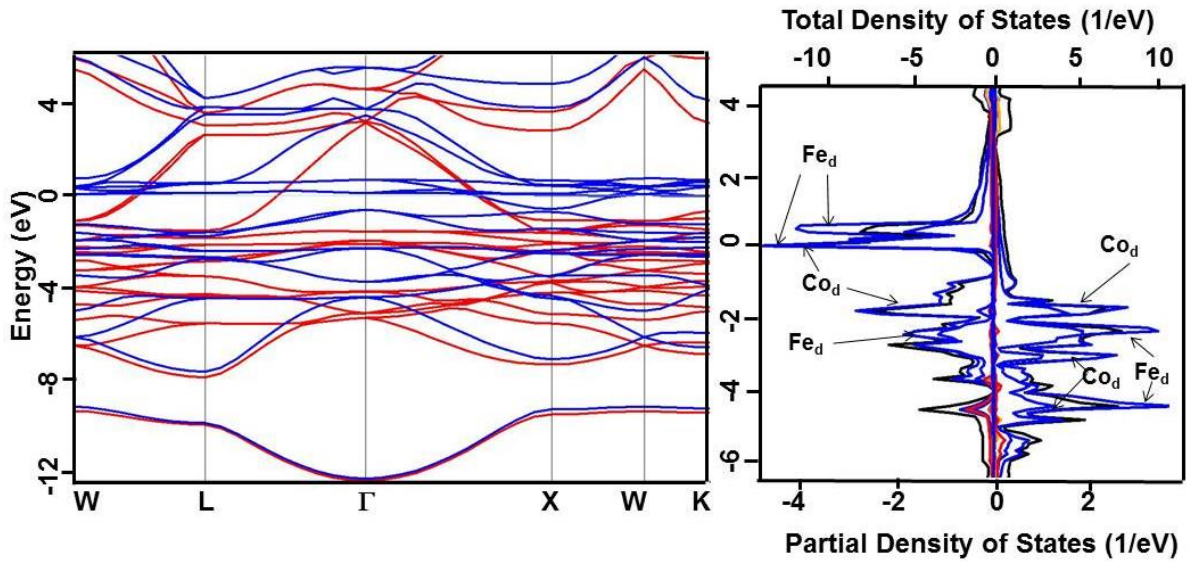


Fig 5 (a)

Fig 5(b)

Figure 5. For Co_2FeSi alloy under GGA (a) Band structure. Up and down spin states have been represented using red and blue colours, respectively. (b) Total DOS (black) and partial DOS of individual atoms. Scales on the top and the bottom axes are to be used to read the total and partial DOS, respectively.

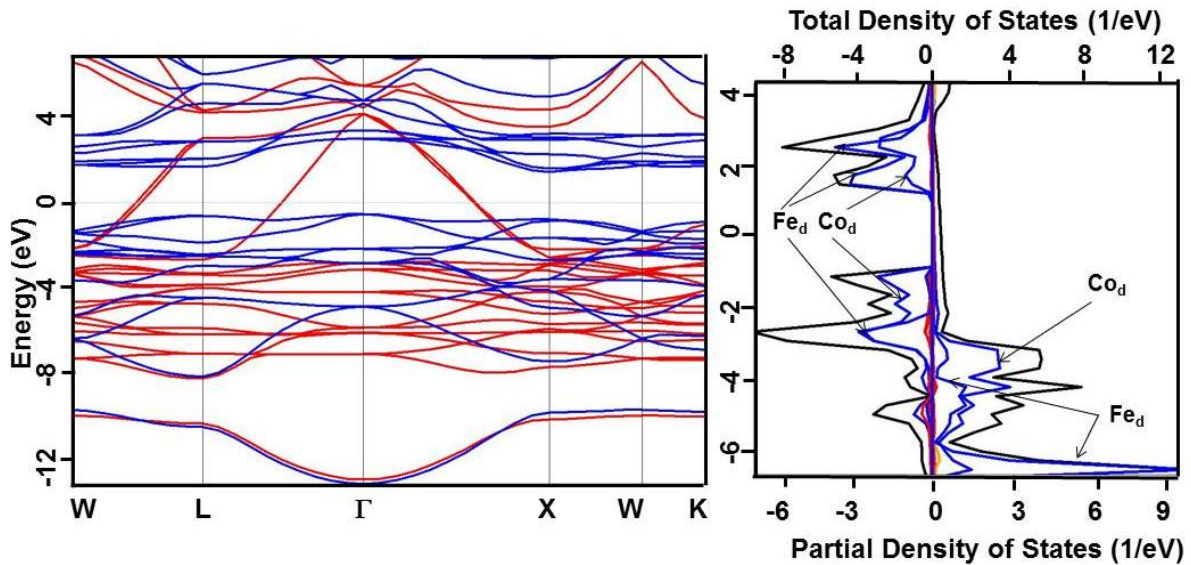


Fig 6 (a)

Fig 6(b)

Figure 6. For Co_2FeSi alloy under HSE approximation (a) Band structure. Up and down spin states have been represented using red and blue colours, respectively. (b) Total DOS (black) and partial DOS of individual atoms. Scales on the top and the bottom axes are to be used to read the total and partial DOS, respectively.

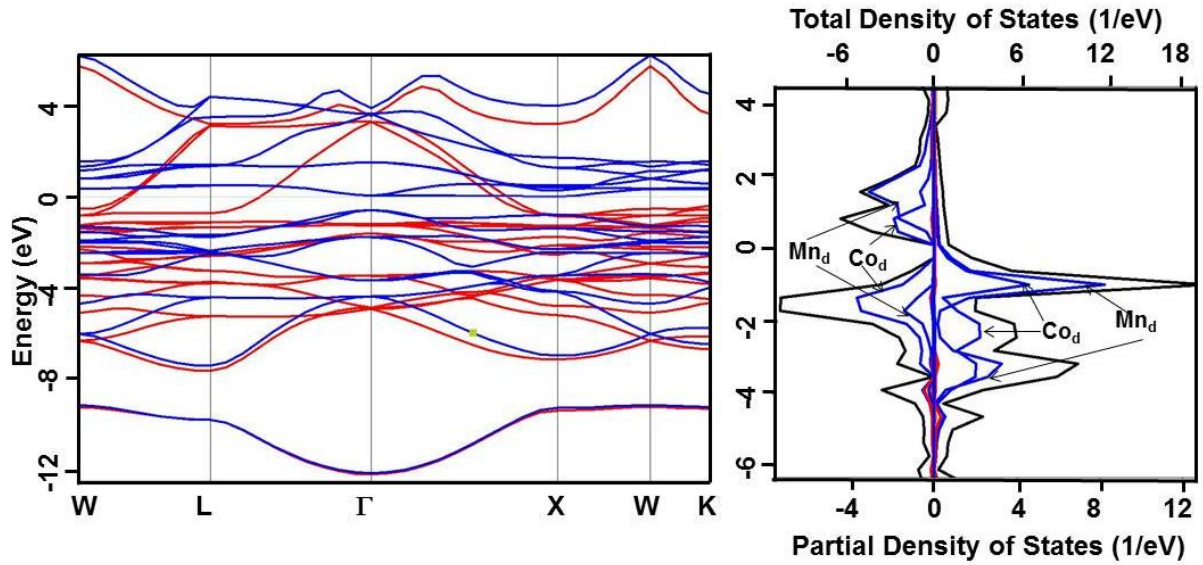


Fig 7 (a)

Fig 7(b)

Figure 7. For Co_2MnSi alloy under GGA (a) Band structure. Up and down spin states have been represented using red and blue colours, respectively. (b) Total DOS (black) and partial DOS of individual atoms. Scales on the top and the bottom axes are to be used to read the total and partial DOS, respectively.

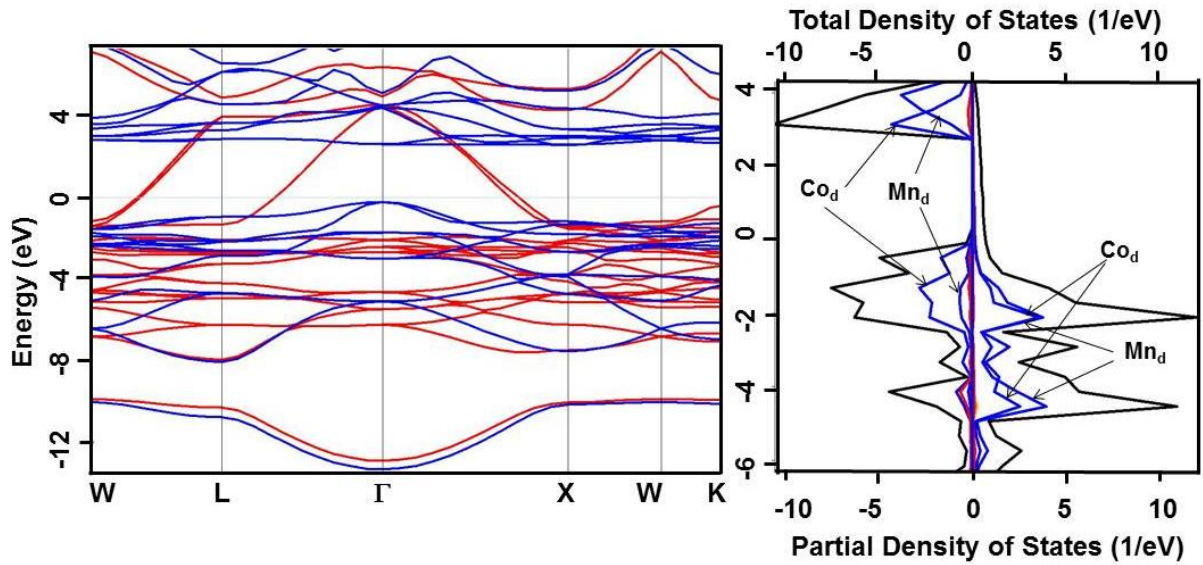


Fig 8 (a)

Fig 8(b)

Figure 8. For Co_2MnSi alloy under HSE approximation (a) Band structure. Up and down spin states have been represented using red and blue colours, respectively. (b) Total DOS (black) and partial DOS of individual atoms. Scales on the top and the bottom axes are to be used to read the total and partial DOS, respectively.

Table 3. Calculated energy gap (E_g) (using GGA, GW_0 , MBJ and HSE06) in spin up and spin down polarization at fermi level (E_f) for Co_2MSi ($M=Cr, Mn, Fe$) for the $\Gamma-\Gamma$ site symmetry. The experimental and other available theoretical values are also given for comparison (Antonov et al., 2008; Alhaj et al., 2013; Chen et al., 2006; Guezlane et al., 2016; Kandpal et al., 2006; Rai et al., 2011; Seema et al., 2015).

System		$E_g\uparrow$ (eV)	$E_g\downarrow$ (eV)			
			GGA	GW_0	mbJ	HSE06
Co_2CrSi	Present study	0.0	0.780	0.860	1.25	2.93
	Others	0.0	0.910 ^a			
		0.0	0.563 ^f			
		0.0	0.720 ^g			
		0.0	0.91 ^b		1.63 ^b	
		0.0	0.87 ^c			
Co_2MnSi	Present study	0.0	0.720	0.840	1.74	2.78
	Others	0.0	0.760 ^d			
		0.0	0.82 ^c			
Co_2FeSi	Present study	0.0	0.680	0.820	1.95 0.86 (X-X)	3.50 2.23 (X-X)
		0.0	1.000 ^e			
	Others	0.0	0.94 ^b		1.77 ^b	

Ref.

^a (Rai et al., 2011)

^b (Guezlane et al., 2016)

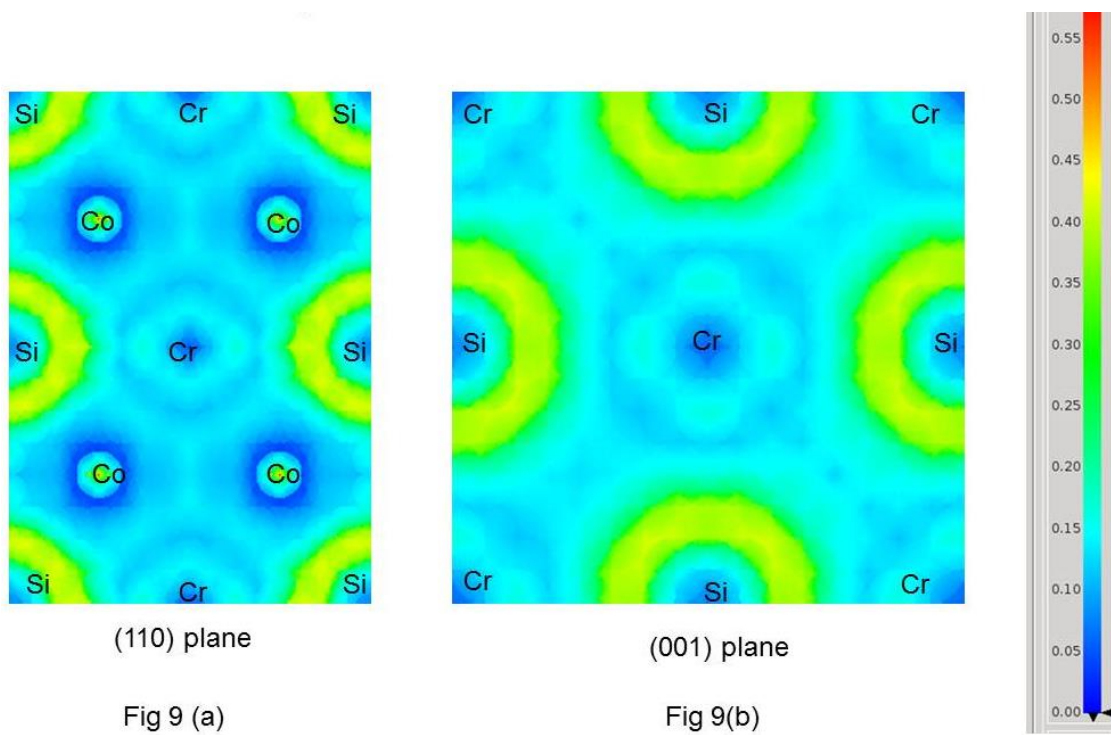
^c (Alhaj et al., 2013)

^d (Antonov et al., 2008)

^e (Kandpal et al., 2006)

^f (Seema et al., 2015)

^g (Chen et al., 2006)



(110) plane

(001) plane

Fig 9 (a)

Fig 9(b)

Figure 9. Two-dimensional (2D) charge density for the Co_2CrSi alloy in (001) and (110) plane.

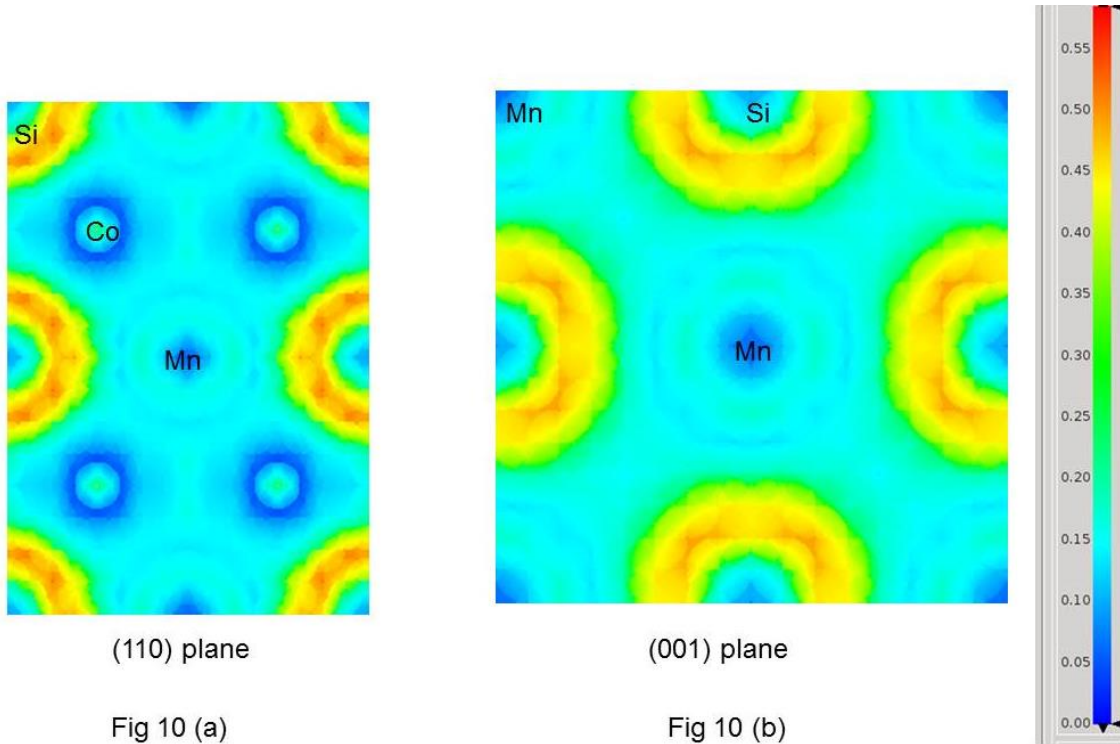


Figure 10. Two-dimensional (2D) charge density for the Co₂MnSi alloy in (001) and (110) plane.

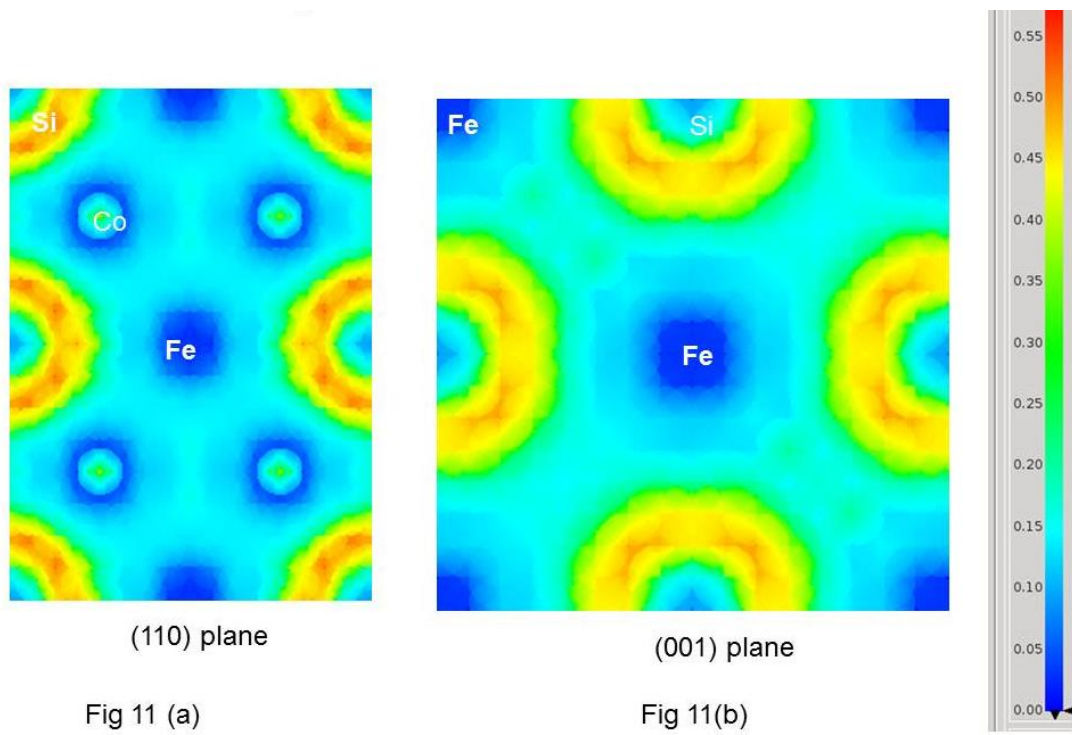


Figure 11. Two-dimensional (2D) charge density for the Co₂FeSi alloy in (001) and (110) plane.

Table 4. Calculated single crystal elastic constants (C_{ij}) and anisotropy factor (A) for Co₂MSi (M= Cr, Mn, Fe).

System		C ₁₁ (GPa)	C ₁₂ (GPa)	C ₄₄ (GPa)	A
Co ₂ CrSi	Present study	303	197	159	3.00
Co ₂ MnSi	Present study	222	170	124	4.73
Co ₂ FeSi	Present study	248	183	113	3.42

Table 5. Calculated values of Cauchy pressures (C_p) and Born stability criteria (BSC) for Co₂MSi (M= Cr, Mn, Fe).

system	C _p (GPa)	(BSC) ₁ (GPa)	(BSC) ₂ (GPa)	(BSC) ₃ (GPa)
Co ₂ CrSi	38	159	106	696
Co ₂ MnSi	47	123	52	562
Co ₂ FeSi	69	113	66	612

The effective elastic modulus of polycrystalline cubic materials can be evaluated from the elastic constants by following two approximations namely, the [Voigt \(1928\)](#) and [Reuss \(1929\)](#) that provide information about the upper and lower limits of modulus. These are defined as

$$B = B_V = B_R = \frac{C_{11} + 2C_{12}}{3} \tag{6}$$

$$G_V = \frac{C_{11} - C_{12} + 3C_{44}}{5} \tag{7}$$

$$G_R = \frac{5(C_{11} - C_{12})C_{44}}{4C_{44} + 3(C_{11} - C_{12})} \tag{8}$$

where B is bulk modulus while G_V and G_R are shear modulus values obtained by Voigt and Reuss approximations, respectively.

The average value of these two estimates mentioned above is given by [Hill \(1952\)](#) approximation for cubic, hexagonal and orthorhombic materials. The Voigt-Reuss-Hill (VRH) average values are given by

$$B = B_H = \frac{B_V + B_R}{2} \tag{9}$$

$$G = G_H = \frac{G_V + G_R}{2} \tag{10}$$

$$E = \frac{9BG}{3B+G} \tag{11}$$

$$\nu = \frac{3B-2G}{2(3B+G)} \tag{12}$$

where, B (=B_H), G (=G_H), E and ν are bulk modulus, shear modulus, Young's modulus and Poisson's ratio, respectively.

The calculated values of B, G and E for these alloys ([Table 6](#)) exhibit maximum value for Co₂CrSi followed by Co₂FeSi and Co₂MnSi alloys. The calculated values for B for all the three alloys are in close agreement with the previously theoretically reported values ([Alhaj et al., 2013](#); [Amari et al., 2016](#)). It is to be noted that the B value for Co₂FeSi is also in good agreement with the experimentally obtained value ([Garg & Vijayakumar, 2011](#)). The calculated values of Poisson's ratio (ν) shows maximum value for Co₂CrSi followed by Co₂MnSi and Co₂FeSi alloys.

The values of B and G can also be utilized for the brittle and ductile behavior of materials ([Pugh, 1954](#)). This can be predicted by taking the ratio G/B. The ratio (G/B) > 0.57 is associated with brittleness. Present calculation clearly indicates that all the three alloys in present study are ductile.

Table 6. Polycrystalline mechanical properties such as Bulk modulus (B), Shear Modulus (G), Young's modulus (E), G/B ratio and Poisson's ratio (ν) for Co_2MSi (M= Cr, Mn, Fe). The other available experimental and theoretical values are also given for comparison (Alhaj et al., 2013; Amari et al., 2016; Garg & Vijayakumar, 2011).

system		B (GPa)	G_V (GPa)	G_R (GPa)	G (GPa)	E (GPa)	ν	G/B
Co ₂ CrSi	Present study	223	117	88	103	267	0.300	0.442
	Others	239 ^a						
Co ₂ MnSi	Present study	187	85	49	67	178	0.340	0.358
	Others	227 ^a						
Co ₂ FeSi	Present study	205	81	57	69	186	0.349	0.338
	Others	204 ^b , 210 ^b						
	Expt.	240 ^c						

4. Conclusions

1. Structural stability and mechanical properties of Co_2MSi (M= Cr, Mn, Fe) Heusler alloys in L_{21} structure have been investigated using DFT within GGA.
2. The lattice constant of these alloys show close values with the previously reported experimental and theoretical data, respectively.
3. The magnetic moment (m) values obtained in present study (using GGA, G_{W0} , mBJ and HSE methods) for all alloys are in accordance with Slater-Pauling rule.
4. All the alloys have predominantly metallic bonding.
5. These alloys are half-metallic as well as ferromagnetic as inferred from their band structure and density of states (DOS).
6. All the three alloys are anisotropic. The extent of anisotropy is highest for Co_2MnSi followed by Co_2FeSi and Co_2CrSi alloys.
7. All the three alloys obey the Born stability criteria and are associated with a ductile behavior based on G/B ratios.

Conflict of interest

The authors have no conflict of interest to declare.

Acknowledgments

Authors are grateful to Defence Research and Development Organization (DRDO) for support and Director, Defence Metallurgical Research Laboratory (DMRL) for his encouragement to carry out this work.

Financing

The authors received no specific funding for this work.

References

- Alhaj, B. A., Hamad, B., Khalifeh, J., & Shaltaf, R. (2013). Ab-initio calculations of the electronic and magnetic structures of $\text{Co}_2\text{Cr}_{1-x}\text{Mn}_x\text{Si}$ alloys. *Journal of Magnetism and Magnetic Materials*, 336, 37-43.
<https://doi.org/10.1016/j.jmmm.2013.02.026>
- Amari, S., Dahmane, F., Omran, S. B., Doumi, B., Yahiaoui, I. E., Tadjer, A., & Khenata, R. (2016). Theoretical investigation of the structural, magnetic and band structure characteristics of $\text{Co}_2\text{FeGe}_{1-x}\text{Si}_x$ ($x=0, 0.5, 1$) full-Heusler alloys. *Journal of the Korean Physical Society*, 69(9), 1462-1468.
<https://doi.org/10.3938/jkps.69.1462>
- Antonov, V. N., Kukusta, D. A., Shpak, A. P., & Yaresko, A. N. (2008). Electronic structure and x-ray magnetic circular dichroism in the Heusler alloy Co_2FeSi . *Condensed Matter Physics*.
- Born, M. (1940). On the stability of crystal lattices. I. In *Mathematical Proceedings of the Cambridge Philosophical Society* (Vol. 36, No. 2, pp. 160-172). Cambridge University Press.
<https://doi.org/10.1017/S0305004100017138>
- <https://www.materialsdesign.com/medea-software>;
<https://www.vasp.at>
- Chen, X. Q., Podloucky, R., & Rogl, P. (2006). Ab initio prediction of half-metallic properties for the ferromagnetic Heusler alloys $\text{Co}_2\text{M}_2\text{Si}$ (M= Ti, V, Cr). *Journal of applied physics*, 100(11), 113901.
<https://doi.org/10.1063/1.2374672>

- Fedorov, F. I. (1968). *Theory of elastic waves in crystals*, New York: Plenum.
- Galanakis, I., & Mavropoulos, P. (2007). Spin-polarization and electronic properties of half-metallic Heusler alloys calculated from first principles. *Journal of Physics: Condensed Matter*, 19(31), 315213.
<https://doi.org/10.1088/09538984/19/31/315213>
- Garg, A. B., & Vijayakumar, V. (2011). Phase stability of Heusler compound Co_2FeSi under pressure: An in-situ x-ray diffraction investigation. *Journal of Applied Physics*, 110(8), 083523.
<https://doi.org/10.1063/1.3656983>
- Graf, T., Felser, C., & Parkin, S. S. (2011). Simple rules for the understanding of Heusler compounds. *Progress in solid state chemistry*, 39(1), 1-50.
<https://doi.org/10.1016/j.progsolidstchem.2011.02.001>
- Guezlane, M., Baaziz, H., Hassan, F. E. H., Charifi, Z., & Djaballah, Y. (2016). Electronic, magnetic and thermal properties of $\text{Co}_2\text{Cr}_x\text{Fe}_{1-x}\text{X}$ (X= Al, Si) Heusler alloys: First-principles calculations. *Journal of Magnetism and Magnetic Materials*, 414, 219-226.
<https://doi.org/10.1016/j.jmmm.2016.04.056>
- Hazra, B. K., Raja, M. M., & Srinath, S. (2016). Correlation between structural, magnetic and transport properties of Co_2FeSi thin films. *Journal of Physics D: Applied Physics*, 49(6), 065007.
- Hedin, L. (1965). New method for calculating the one-particle Green's function with application to the electron-gas problem. *Physical Review*, 139(3A), A796.
<https://doi.org/10.1103/PhysRev.139.A796>
- Heyd, J., Scuseria, G. E., & Ernzerhof, M. (2003). Hybrid functionals based on a screened Coulomb potential. *The Journal of chemical physics*, 118(18), 8207-8215.
<https://doi.org/10.1063/1.1564060>
- Hill, R. (1952). The elastic behaviour of a crystalline aggregate. *Proceedings of the Physical Society. Section A*, 65(5), 349.
<https://doi.org/10.1088/0370-1298/65/5/307>
- Hohenberg, P., & Kohn, W. (1964). Inhomogeneous electron gas. *Physical review*, 136(3B), B864.
<https://doi.org/10.1103/PhysRev.136.B864>
- Kandpal, H. C., Fecher, G. H., Felser, C., & Schönhense, G. (2006). Correlation in the transition-metal-based Heusler compounds Co_2MnSi and Co_2FeSi . *Physical Review B*, 73(9), 094422.
<https://doi.org/10.1103/PhysRevB.73.094422>
- Kandpal, H. C., Fecher, G. H., & Felser, C. (2007). Calculated electronic and magnetic properties of the half-metallic, transition metal based Heusler compounds. *Journal of Physics D: Applied Physics*, 40(6), 1507.
<https://doi.org/10.1088/0022-3727/40/6/s01>
- Kohn, W., & Sham, L. J. (1965). Self-consistent equations including exchange and correlation effects. *Physical review*, 140(4A), A1133.
<https://doi.org/10.1103/PhysRev.140.A1133>
- Kumar, M., Nautiyal, T., & Auluck, S. (2009). First-principles calculations of electronic and optical properties of $\text{Fe}_{3-x}\text{V}_x\text{Al}$ (x= 0–3) compounds. *Journal of Physics: Condensed Matter*, 21(44), 446001.
<https://doi.org/10.1088/0953-8984/21/44/446001>
- Luo, H., Zhu, Z., Ma, L., Xu, S., Liu, H., Qu, J., ... & Wu, G. (2007). Electronic structure and magnetic properties of Fe_2YSi (Y= Cr, Mn, Fe, Co, Ni) Heusler alloys: a theoretical and experimental study. *Journal of Physics D: Applied Physics*, 40(22), 7121.
<https://doi.org/10.1088/0022-3727/40/22/039>
- Mohankumar, R., Ramasubramanian, S., Rajagopalan, M., Manivel Raja, M., Kamat, S. V., & Kumar, J. (2015). Density functional study of half-metallic property on B_2 disordered Co_2FeSi . *Journal of Materials Science*, 50(3), 1287-1294.
<https://doi.org/10.1007/s10853-014-8687-0>
- Monkhorst, H. J., & Pack, J. D. (1976). Special points for Brillouin-zone integrations. *Physical review B*, 13(12), 5188.
<https://doi.org/10.1103/PhysRevB.13.5188>
- Niculescu, V., Burch, T. J., Raj, K., & Budnick, J. I. (1977). Properties of Heusler-type materials Fe_2TSi and FeCo_2Si . *Journal of Magnetism and Magnetic Materials*, 5(1), 60-66.
[https://doi.org/10.1016/0304-8853\(77\)90197-4](https://doi.org/10.1016/0304-8853(77)90197-4)
- Pauling, L. (1938). The nature of the interatomic forces in metals. *Physical Review*, 54(11), 899.
<https://doi.org/10.1103/PhysRev.54.899>

- Perdew, J. P., Burke, K., & Ernzerhof, M. (1996). Generalized gradient approximation made simple. *Physical review letters*, 77(18), 3865.
<https://doi.org/10.1103/PhysRevLett.77.3865>
- Pettifor, D., & Aoki, M. (1991). Bonding and structure of intermetallics: a new bond order potential. *Materials Science. Philosophical Transactions of the Royal Society of London. Series A: Physical and Engineering Sciences*, 334, 1635
<https://doi.org/10.1098/rsta.1991.0024>
- Pugh, S. F. (1954). XCII. Relations between the elastic moduli and the plastic properties of polycrystalline pure metals. *The London, Edinburgh, and Dublin Philosophical Magazine and Journal of Science*, 45(367), 823-843.
<https://doi.org/10.1080/14786440808520496>
- Rai, D. P., Ghimire, M. P., & Thapa, R. K. (2011). Study of energy bands and magnetic properties of Co₂CrSi Heusler alloy. *Bulletin of Materials Science*, 34(6), 1219-1222.
<https://doi.org/10.1007/s12034-011-0233-y>
- Ramudu, M., Manivel Raja, M. & Kamat, S.V. (2015). Effect of boron on the structural and magnetic properties of Co₂FeSi_{1-x}B_x Heusler alloys. *DAE Solid State Physics Symposium*.
<https://doi.org/10.1063/1.4948123>
- Raphael, M. P., Ravel, B., Huang, Q., Willard, M. A., Cheng, S. F., Das, B. N., ... & Harris, V. G. (2002). Presence of antisite disorder and its characterization in the predicted half-metal Co₂MnSi. *Physical Review B*, 66(10), 104429.
<https://doi.org/10.1103/PhysRevB.66.104429>
- Reuss, A. (1929). Calculation of the bulk modulus of polycrystalline materials. *Ztschr Angew Math Mech*, 9, 49.
<https://doi.org/10.1002/zamm.19290090104>
- Seema, K., Umran, N. M., & Kumar, R. (2015). Effect of Disorder on Electronic, Magnetic, and Optical Properties of Co₂CrZ Heusler Alloys (Z= Al, Ga, Si, Ge). *Journal of Superconductivity and Novel Magnetism*, 29(2), 401-408.
<https://doi.org/10.1007/s10948-015-3271-7>
- Slater, J. C. (1936). The ferromagnetism of nickel. II. Temperature effects. *Physical Review*, 49(12), 931.
<https://doi.org/10.1103/PhysRev.49.931>
- Tran, F., & Blaha, P. (2009). Accurate band gaps of semiconductors and insulators with a semilocal exchange-correlation potential. *Physical review letters*, 102(22), 226401.
<https://doi.org/10.1103/PhysRevLett.102.226401>
- Umetsu, R. Y., Okubo, A., Xu, X., & Kainuma, R. (2014). Magnetic properties and phase stability of Co₂Cr (Ga, Si) Heusler alloys. *Journal of alloys and compounds*, 588, 153-157.
<https://doi.org/10.1016/j.jallcom.2013.10.209>
- Voigt, W. (1928). *Lehrburch der Kristallphysik*, Teubner, Leipzig.
- Wurmehl, S., Fecher, G. H., Kandpal, H. C., Ksenofontov, V., Felser, C., Lin, H. J., & Morais, J. (2005). Geometric, electronic, and magnetic structure of Co₂FeSi: Curie temperature and magnetic moment measurements and calculations. *Physical Review B*, 72(18), 184434.
<https://doi.org/10.1103/PhysRevB.72.184434>
- Yin, M., Chen, S., & Nash, P. (2013). Enthalpies of formation of selected Co₂YZ Heusler compounds. *Journal of alloys and compounds*, 577, 49-56.
<https://doi.org/10.1016/j.jallcom.2013.04.136>
- Zhu, X., Wang, Y., Wang, L., Dai, Y., & Luo, C. (2014). Pressure and disorder effects on the half-metallic character and magnetic properties of the full-Heusler alloy Co₂FeSi. *Journal of Physics and Chemistry of Solids*, 75(3), 391-396.
<https://doi.org/10.1016/j.jpccs.2013.11.008>